

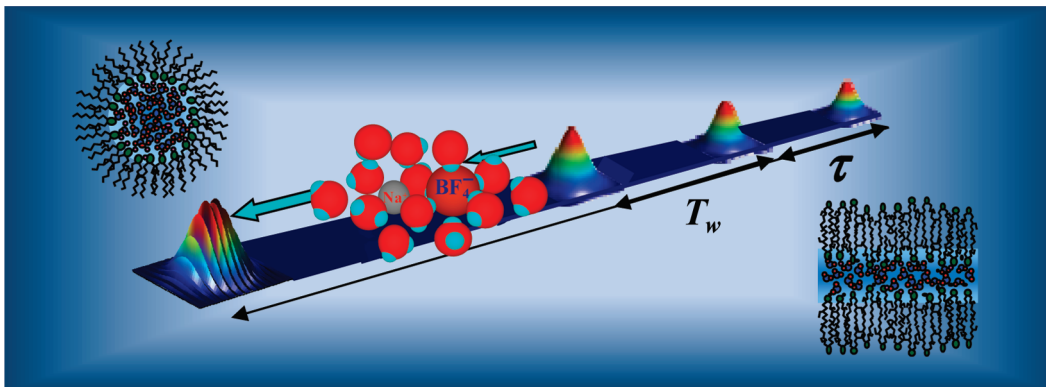
# Dynamics of Water Interacting with Interfaces, Molecules, and Ions.

MICHAEL D. FAYER

Department of Chemistry, Stanford University, Stanford, California 94305,  
United States

RECEIVED ON JANUARY 10, 2011

## CONSPECTUS



Water is a critical component of many chemical processes, in fields as diverse as biology and geology. Water in chemical, biological, and other systems frequently occurs in very crowded situations: the confined water must interact with a variety of interfaces and molecular groups, often on a characteristic length scale of nanometers. Water's behavior in diverse environments is an important contributor to the functioning of chemical systems. In biology, water is found in cells, where it hydrates membranes and large biomolecules. In geology, interfacial water molecules can control ion adsorption and mineral dissolution. Embedded water molecules can change the structure of zeolites. In chemistry, water is an important polar solvent that is often in contact with interfaces, for example, in ion-exchange resin systems.

Water is a very small molecule; its unusual properties for its size are attributable to the formation of extended hydrogen bond networks. A water molecule is similar in mass and volume to methane, but methane is a gas at room temperature, with melting and boiling points of 91 and 112 K, respectively. This is in contrast to water, with melting and boiling points of 273 and 373 K, respectively. The difference is that water forms up to four hydrogen bonds with approximately tetrahedral geometry. Water's hydrogen bond network is not static. Hydrogen bonds are constantly forming and breaking. In bulk water, the time scale for hydrogen bond randomization through concerted formation and dissociation of hydrogen bonds is approximately 2 ps. Water's rapid hydrogen bond rearrangement makes possible many of the processes that occur in water, such as protein folding and ion solvation. However, many processes involving water do not take place in pure bulk water, and water's hydrogen bond structural dynamics can be substantially influenced by the presence of, for example, interfaces, ions, and large molecules. In this Account, spectroscopic studies that have been used to explore the details of these influences are discussed.

Because rearrangements of water molecules occur so quickly, ultrafast infrared experiments that probe water's hydroxyl stretching mode are useful in providing direct information about water dynamics on the appropriate time scales. Infrared polarization-selective pump–probe experiments and two-dimensional infrared (2D IR) vibrational echo experiments have been used to study the hydrogen bond dynamics of water. Water orientational relaxation, which requires hydrogen bond rearrangements, has been studied at spherical interfaces of ionic reverse micelles and compared with planar interfaces of lamellar structures composed of the same surfactants. Water orientational relaxation slows considerably at interfaces. It is found that the geometry of the interface is less important than the presence of the interface. The influence of ions is shown to slow hydrogen bond rearrangements. However, comparing an ionic interface to a neutral interface demonstrates that the chemical nature of the interface is less important than the presence of the interface. Finally, it is found that the dynamics of water at an organic interface is very similar to water molecules interacting with a large polyether.

## I. Introduction

Water's ability to act as a unique venue for chemical processes is related to its formation of extended hydrogen bond networks. A water molecule can make up to four hydrogen bonds with other water molecules, forming an approximately tetrahedral structure. In pure bulk water, the hydrogen bond network is constantly evolving over a range of time scales, from tens of femtoseconds to picoseconds.<sup>1,2</sup> Hydrogen bonds are continually forming and breaking through concerted hydrogen bond rearrangements.<sup>3</sup> These dynamical processes can be observed on the time scales on which they take place using ultrafast infrared spectroscopy.<sup>1,2,4–8</sup> Orientational relaxation of pure water (2.6 ps)<sup>9</sup> occurs through concerted hydrogen bond rearrangement.<sup>3</sup>

When water comes in contact with interfaces, ions, or large molecules, the dynamics of the hydrogen bonding network change.<sup>10–17</sup> There are a number of important questions concerning water's interactions with other species. How much does the interaction of water with an interface, ion, or large molecule influence water dynamics?<sup>8,13,18</sup> If water is interacting with an interface, does the geometry of the interface matter?<sup>11</sup> Is there a substantial difference between the dynamics of water interacting with a charged versus neutral interface?<sup>19,20</sup>

Here ultrafast infrared experiments are employed to shed light on these issues. IR polarization selective pump–probe experiments are used to measure the orientational relaxation of water in a variety of systems. Orientational relaxation requires hydrogen bond rearrangement. For a water molecule to reorient, it must break and reform hydrogen bonds in what is referred to as jump reorientation.<sup>3</sup> Thus, orientational relaxation provides information on the dynamics of the hydrogen bond network and how it is affected by interactions with interfaces and large molecules. Ultrafast 2D IR vibrational echo experiments are used to measure the chemical exchange between water hydrogen bonded to an ion and water hydrogen bonded to another water molecule. The 2D IR chemical exchange experiments provide a direct measurement on the influence of ions on hydrogen bond switching.

## II. Experimental Procedures

The OD hydroxyl stretching mode of dilute HOD in H<sub>2</sub>O was studied. The OD stretch is used to eliminate vibrational excitation transfer, which can cause artificial decay of the orientational correlation function.<sup>23,24</sup> MD simulations of HOD in bulk H<sub>2</sub>O demonstrate that dilute HOD does not

change the properties of water, and the dynamics of HOD report on the dynamics of water.<sup>4</sup>

The laser system used for these experiments consists of a Ti:Sapphire oscillator and regenerative amplifier pumping an OPA and difference frequency stage to produce ~60 fs pulses at ~4 μm (2500 cm<sup>-1</sup>). Two types of pulse sequences are used for the polarization-selective pump–probe experiments and the 2D IR vibrational echo experiments. For the pump–probe experiments, the mid-IR light was split into an intense pump pulse and a weak probe pulse. Immediately before the sample, the polarization of the pump pulse is rotated from horizontal to 45° relative to the horizontally polarized probe. The polarization of the probe is resolved parallel and perpendicular to the pump (+45° and –45° relative to vertical) after the sample using a computer controlled rotation stage. The probe is frequency dispersed by a monochromator and detected using a 32 element MCT array detector.

The pump–probe signal measured parallel ( $I_{\parallel}$ ) and perpendicular ( $I_{\perp}$ ) to the pump polarization contains information about both the population relaxation and the orientational dynamics of the HOD molecules.

$$I_{\parallel} = P(t)(1 + 0.8C_2(t)) \quad (1)$$

$$I_{\perp} = P(t)(1 - 0.4C_2(t)) \quad (2)$$

$P(t)$  is the vibrational population relaxation, and  $C_2(t)$  is the second Legendre polynomial orientational correlation function. Pure population relaxation can be extracted from the parallel and perpendicular signals using

$$P(t) = I_{\parallel} + 2I_{\perp} \quad (3)$$

In the case of a single ensemble of molecules undergoing orientational relaxation, the orientational correlation function,  $C_2(t)$ , can be determined from the anisotropy,  $r(t)$ , by

$$r(t) = (I_{\parallel} - I_{\perp})/(I_{\parallel} + 2I_{\perp}) = 0.4C_2(t) \quad (4)$$

When multiple ensembles are present in a system, the population relaxation given in eq 3 is a weighted sum of the population relaxation of the ensembles. The expression for the anisotropy, eq 4, becomes much more complicated. These complications and methods for extracting the orientational correlation function in two ensemble systems have been discussed in detail previously<sup>10,12,13</sup> and will be briefly discussed below.

In the 2D IR vibrational echo experiments,<sup>25</sup> the IR beam is split into three excitation pulses and a fourth beam, the

local oscillator (LO). The three excitation pulses are time ordered, with pulses 1 and 2 traveling along variable delay stages. The first pulse creates a coherence consisting of a superposition of the  $v=0$  and  $v=1$  vibrational levels. During the evolution period  $\tau$ , the phase relationships between the oscillators decay. The second pulse reaches the sample at time  $\tau$  and creates a population state in either  $v=0$  or  $v=1$ . A time  $T_w$  (the waiting period) elapses before the third pulse arrives at the sample to create another coherence that partially restores the phase relationships. Rephasing of the oscillators causes the vibrational echo signal to be emitted at a time  $t \leq \tau$  after the third pulse. During  $T_w$ , the water molecules sample different environments due to dynamic structural evolution of the system. The frequencies of the OD vibrational oscillators change (spectral diffusion<sup>1,4,26,27</sup> or chemical exchange<sup>8,28,29</sup>) as the water network structure changes. The vibrational echo signal is spatially and temporally overlapped with the LO for heterodyned detection, which provides both amplitude and phase information. The heterodyned signal is frequency dispersed by a monochromator and detected with the 32 element array detector. At a fixed  $T_w$ ,  $\tau$  is scanned to generate a 2D IR vibrational echo spectrum. To obtain a 2D spectrum, two Fourier transforms are necessary. Taking the spectrum of the heterodyned signal provides one of the Fourier transforms giving the vertical axis ( $\omega_m$  axis) in the 2D spectrum. At each  $\omega_m$  frequency, scanning  $\tau$  produces a temporal interferogram. Numerical Fourier transforms of these interferograms give the horizontal axis ( $\omega_\tau$  axis). Then  $T_w$  is changed, and another 2D spectrum is recorded. The time evolution of the 2D spectra provides the information on the system dynamics.

### III. Results and Discussion

**A. Water Dynamics at the Interface of AOT Reverse Micelles.** Ultrafast infrared spectroscopy has been used to study water in a variety of nanoconfined systems, in which the dynamics of water are dominated by the effects of the interface.<sup>10–12,14,19–22</sup> Many of these studies have focused on the dynamics of water confined in reverse micelles formed by the surfactant aerosol-OT (sodium bis(2-ethylhexyl) sulfosuccinate). AOT forms well-characterized nominally mono-dispersed spherical reverse micelles in isoctane and other organic solvents over a large range of water content from essentially dry up to  $\sim 60$  water molecules per AOT.<sup>30</sup> Figure 1 shows schematic illustrations of a reverse micelle. The number of water molecules per AOT is conveniently described using

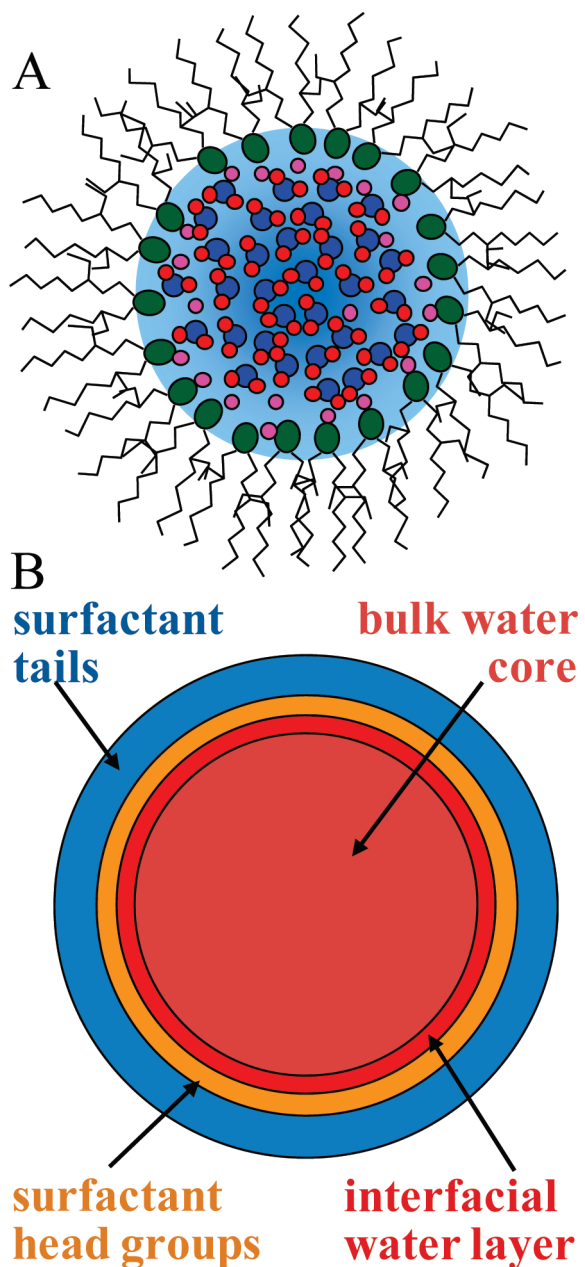
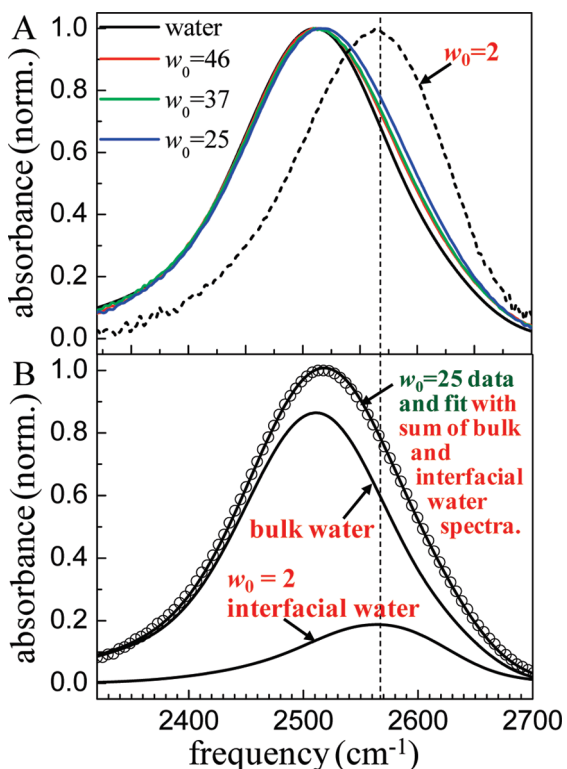


FIGURE 1. (A) Diagram of AOT reverse micelle. (B) Schematic showing the various regions of the reverse micelle structure.

the  $w_0$  parameter,  $w_0 = [\text{H}_2\text{O}]/[\text{AOT}]$ . The smallest reverse micelles have radii of less than 1 nm (50–100 waters), while the largest have radii of up to 14 nm ( $\sim 400\,000$  waters). With this large size range, it is possible to change the relative amount of the water interacting directly with the interface from a large fraction to a small fraction of the total by increasing the reverse micelle size.

The properties of water confined in relatively large AOT reverse micelles can be described using a core/shell model in which a shell of water molecules interacting directly with the interface have an absorption spectrum, vibrational



**FIGURE 2.** (A) Spectra of the OD stretch of HOD in H<sub>2</sub>O in bulk water and different size AOT reverse micelles. (B) Spectrum (circles) with fit through circles (solid curve). The fit is the weighted sum of the bulk water spectrum and the  $w_0 = 2$  spectrum, which is a model for interfacial water.

lifetime, and orientational dynamics that are distinct from the more bulk-like water found in the center of the reverse micelle water pool.<sup>10–12,14,19,31</sup>

First, the dynamics of the orientational relaxation of water molecules directly in contact with the interfaces of large reverse micelles will be discussed. Large reverse micelles ( $w_0 = 46, 37$ , and  $25$  with radii =  $10, 8.5$ , and  $4.5$  nm) are useful for this type of study to ensure that a significant bulk-like water pool exists in the center (see Figure 1). Laage and Hynes have shown that the orientational dynamics of a water molecule depend on the motions of water molecules in its first and second solvation shell.<sup>3,32</sup> Based on this model, the water in the core of a large reverse micelle should have bulk characteristics because the water is spatially well separated from the interface and has first and second solvation shells that also do not interact with the interface. This criterion does not apply for smaller reverse micelles.<sup>10</sup>

Figure 2 displays absorption spectra of the OD stretch of HOD in H<sub>2</sub>O in several reverse micelles and in bulk water. The reverse micelles with  $w_0 = 46, 37, 25$ , and  $2$  have approximately 150 000, 77 000, 11 500, and 40 water molecules in their water nanopools, respectively. The large reverse micelles

have spectra that are only somewhat different from that of bulk water. As they get smaller, the spectrum shifts to the blue (higher frequency). These spectra are similar to that of bulk water because each has a large core of bulk-like water (see Figure 1B) and a relatively small fraction of water at the interface. In contrast, the spectrum of  $w_0 = 2$  is very different than that of bulk water, with a substantial blue shift, because essentially all of the water molecules are interacting with the interface. The spectrum of  $w_0 = 2$  is used as a model for the interfacial water spectrum. The spectra of the large reverse micelles are composed of a bulk water spectrum and an interfacial spectrum. The blue shift increases as the reverse micelle becomes smaller because a larger fraction of the water is interacting with the interface. Figure 2B shows the spectrum of  $w_0 = 25$  (circles) as well as the spectra of bulk water and  $w_0 = 2$  interfacial water. The solid curve through the circles is the fit to the  $w_0 = 25$  spectrum only adjusting the relative amplitudes of the bulk water and  $w_0 = 2$  water spectra. The fit is clearly very good. The spectra in Figure 2B show that by conducting the time-dependent IR experiments on the blue side of the large reverse micelle spectra, a significant fraction of the data will come from the interfacial water.

Equations 3 and 4 gave the formulas for the contributions to the pump–probe signal when the probe is resolved parallel and perpendicular to the pump. When there is more than one subensemble in a system, the contributions of each subensemble to the signal are additive and the population relaxation is given by the weighted sum of the population relaxation of the two components.<sup>12</sup>

$$P(t) = aP_w(t) + (1 - a)P_{int}(t) \quad (5)$$

Here,  $a$  is a weighting factor and  $P_i(t)$  is the population relaxation of component  $i$ . The factor  $a$  is related to the fractional concentration of the two species at a particular wavelength. The subscript  $w$  stands for water, as the core has the population relaxation time of bulk water (1.8 ps), and  $int$  stands for the interfacial water.

When more than one subensemble is present, the anisotropy decay becomes quite complicated. To see this, the numerator and denominator of eq 4 are written out explicitly.

$$\begin{aligned} r(t) &= \frac{a(l_{||}^w - l_{\perp}^w) + (1 - a)(l_{||}^{int} - l_{\perp}^{int})}{a(l_{||}^w + 2l_{\perp}^w) + (1 - a)(l_{||}^{int} + 2l_{\perp}^{int})} \\ &= 0.4 \frac{aP_w(t)C_2^w(t) + (1 - a)P_{int}(t)C_2^{int}(t)}{aP_w(t) + (1 - a)P_{int}(t)} \end{aligned} \quad (6)$$

The parallel and perpendicular pump–probe signals due to component  $i$  are given by  $I_{||}^i$  and  $I_{\perp}^i$ , respectively, and the

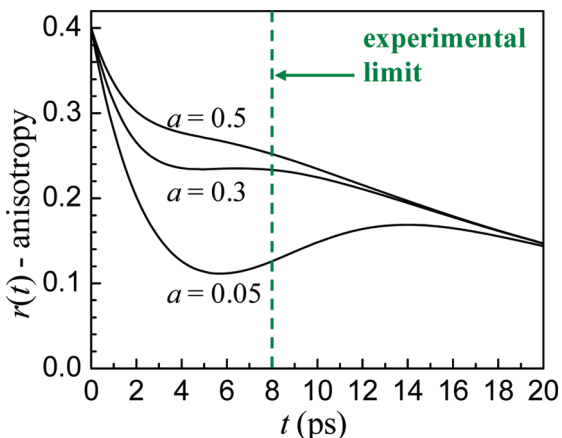


**FIGURE 3.** Model calculations of orientational anisotropy decays for a two-component system, that is, bulk-like water and interfacial water.

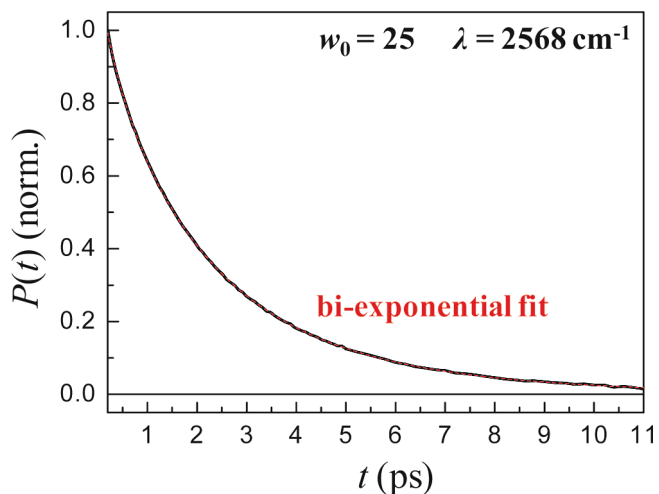


**FIGURE 4.** Population decay data (solid black curve) and a biexponential fit (dashed red curve).

orientational correlation functions are given by  $C_2^i(t)$ . For a single-component system, the population relaxation divides out of the right-hand side of eq 6; with multiple components, the anisotropy decay is not a direct measurement of the orientational correlation function. If the two components have a large separation of time scales for both their vibrational lifetimes and orientational dynamics, then when the fast component has decayed away, the long time anisotropy decay will be an accurate representation of the anisotropy of the slow component. However, at intermediate times, eq 6 is required to extract information about the orientational dynamics. Figure 3 displays model calculations using eq 6 and parameters that are appropriate for the reverse micelle systems (see below). The green dashed line shows limitations imposed

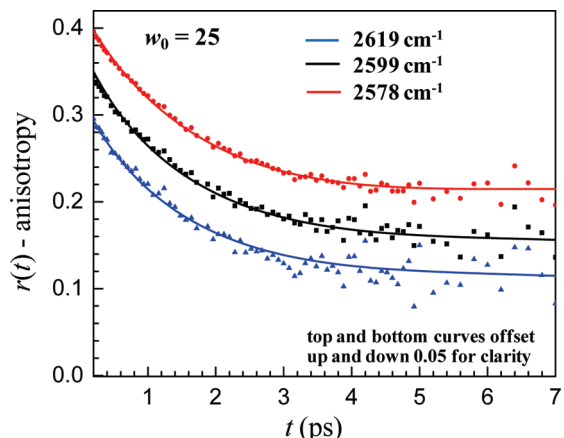


**FIGURE 5.** Water in AOT anisotropy decay data (points) and fits to the two-component model (solid curves) for three wavelengths.

by the OD vibrational lifetimes on how far out in time data can be obtained. The shapes of the curves are very sensitive to the input parameters.

Figure 4 shows a population relaxation data for  $w_0 = 25$  (solid black curve) and a biexponential fit (dashed red curve) using eq 5 at a particular wavelength ( $2568 \text{ cm}^{-1}$ ), which is on the blue side of the absorption line (see Figure 2B). Fits like the one shown are obtained at many wavelengths. These give the lifetimes and the parameters,  $a$ , at each wavelength. In the fit, one component gives the bulk water lifetime, 1.8 ps, at all wavelengths. The other component is also found to be independent of wavelength within experimental error. It is the lifetime of the OD stretch for water molecules interacting with the interface. For  $w_0 = 46$ ,  $37$ , and  $25$ , the interfacial water lifetimes are  $3.9 \pm 0.5$  ps,  $4.6 \pm 0.5$  ps, and  $4.3 \pm 0.5$  ps. Within experimental error, the values are the same, 4.3 ps. This value is used in the subsequent analysis.

Measurements of the orientational relaxation time in bulk water give an exponential decay with an orientational relaxation time constant of 2.6 ps.<sup>12</sup> We now know the lifetimes, the parameters,  $a$ , for each wavelength, and the bulk water orientational relaxation time. In eq 6, the only unknown parameter is the interfacial water orientational relaxation time,  $\tau_{\text{int}}$ . We have the fitting equation

$$r(t) = 0.4 \frac{a e^{-t/1.8} e^{-t/2.6} + (1-a) e^{-t/4.3} e^{-t/\tau_{\text{int}}}}{a e^{-t/1.8} + (1-a) e^{-t/4.3}} \quad (7)$$

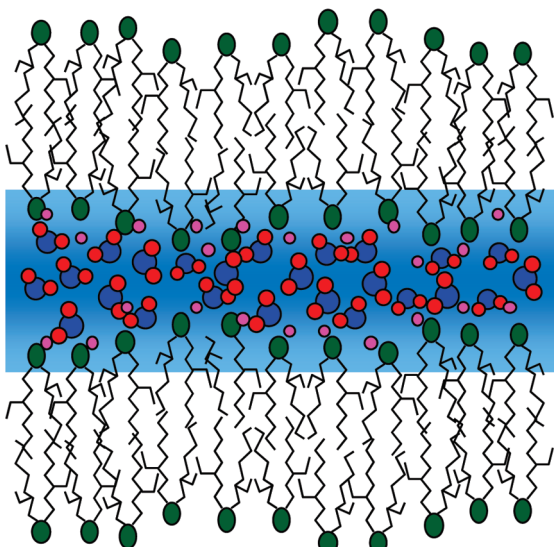
Equation 7 is used to do a global fit to a range of wavelengths to determine the interfacial orientation relaxation time constant,  $\tau_{\text{int}}$ . Because there is only one adjustable parameter and the “plateau level” (see Figure 3) is very sensitive to  $\tau_{\text{int}}$ , by simultaneously fitting many

wavelengths the resulting errors in the fits are relatively small even though the data are fit over a restricted time range. Sample results are shown in Figure 5 for three wavelengths of the  $w_0 = 25$  data.<sup>12</sup> The experiments were conducted on four different sizes of large reverse micelles. Large means that they are sufficiently large to have a core (see Figure 1B) with bulk water characteristics. The results for  $w_0 = 46, 37, 25$ , and  $16.5$  are  $18 \pm 3$  ps,  $18 \pm 3$  ps,  $19 \pm 3$  ps, and  $18 \pm 3$  ps, respectively. Therefore, within experimental error the interfacial orientational relaxation times are independent of size and all are 18 ps. This should be compared with 2.6 ps, the value for bulk water. Interaction with the interface of large spherical AOT reverse micelles slows orientational relaxation substantially.

**B. The Influence of Geometry and Charges.** The results presented above are for spherical AOT reverse micelles. AOT also forms lamellar structures when mixed with water as illustrated in Figure 6. The lamellar structure and repeat distances have been characterized by X-ray diffraction.<sup>33</sup> The identical experiments that were performed on AOT reverse micelles were conducted on lamellar structures having a range of interlayer separations. Figure 7 shows

data for four lamellar samples.<sup>11</sup> Each of these has a slab separation that is sufficiently large that there is a core of bulk

## AOT Lamellar Structure



### 2D slab of water, effectively infinite in two dimensions

FIGURE 6. Diagram of an AOT lamellar structure.

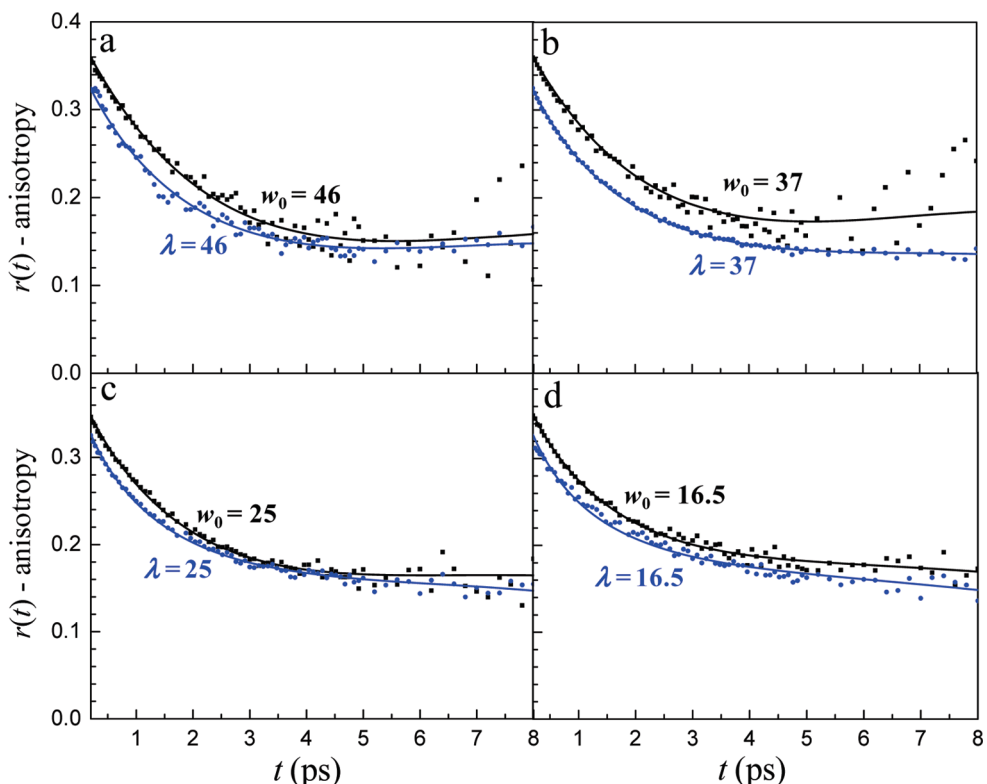
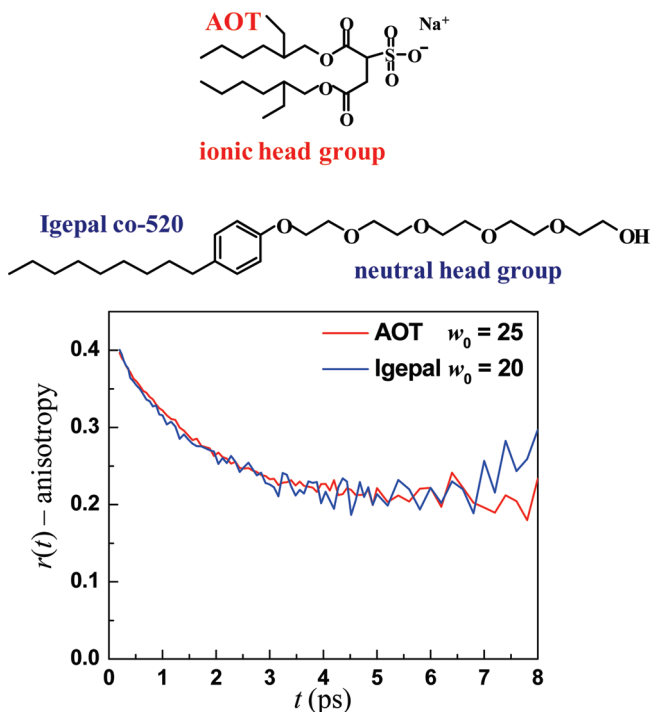


FIGURE 7. A comparison of orientational relaxation data (points) and fits (solid curves) for water in AOT reverse micelles (black, labeled with  $w_0$ ) and AOT lamellar structures (blue, labeled with  $\lambda$ ).



**FIGURE 8.** Top, structures of the charged surfactant AOT and the neutral surfactant Igepal co-520. Bottom, comparison of the water orientational relaxation data for water in AOT and Igepal reverse micelles that have the same diameter water nanopools.

water. The parameter  $\lambda$  is the number of waters per head-group for the lamellar structures, that is, the equivalent of  $w_0$  for the reverse micelles. Figure 7 also shows the reverse micelle data with  $\lambda = w_0$ . As can be seen in the figure, the data are very similar. Fits to the lamellar data using eqs 5 and 6 give the interfacial orientational relaxation times for  $\lambda = 16.5, 25, 37$ , and  $46$  of  $17 \pm 2$  ps,  $18 \pm 3$  ps,  $19 \pm 2$  ps, and  $24 \pm 9$  ps, respectively. Within experimental error, the orientational relaxation times for water at the interfaces of AOT lamellar structures (planar interfaces) are the same as those for the AOT spherical reverse micelles. The important result is that the geometry of the confining nanoscopic structure does not matter so long as the core is large enough to consist of bulk-like water.

Both the AOT reverse micelles and the lamellar structures have the same sulfonate ionic head groups. To determine the role of interfacial charges, reverse micelles formed from the neutral surfactant Igepal co-520 were studied. The Igepal structure is shown in Figure 8. Igepal forms monodispersed, spherical reverse micelles.<sup>34</sup> Igepal  $w_0 = 20$  reverse micelles have the same size water nanopool, that is, a diameter of 9 nm, as  $w_0 = 25$  AOT reverse micelles. Figure 8 shows a comparison of the orientational relaxation data for the two samples.<sup>19</sup> While they are very similar, they are not

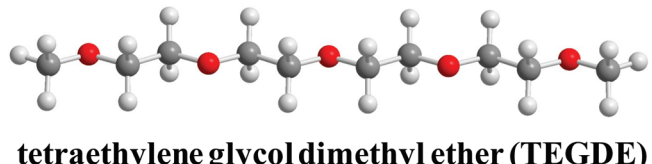


**FIGURE 9.** Top, structure of tetraethylene glycol dimethyl ether (TEGDE). Bottom, orientational relaxation data (red curve) for water in a water/TEGDE solution (50 water molecules per TEGDE) and a fit (blue dashed curve) to the two-component model. Also shown is orientational relaxation data of bulk water (black curve).

identical. The Igepal data has an upturn at long time as in one of the model calculations shown in Figure 3. Fitting the Igepal data as described above gives the interfacial orientation relaxation time. The results are Igepal  $13 \pm 4$  ps, AOT  $18 \pm 3$  ps, and, for comparison, bulk water  $2.6 \pm 0.1$  ps. The orientational relaxation time for water at the nonionic Igepal interface is slightly faster than that of AOT. However, the error bars overlap somewhat. Therefore, it is not certain that they are actually different. Even if they do display some difference, the important point is that going from an ionic interface to a neutral interface at most made a relatively small difference. Therefore, the presence of the interface has a more substantial influence on the orientational relaxation dynamics of water than the chemical nature of the interface for these two very different interfaces.

Water interacting with much larger molecules will also affect water dynamics. Figure 9 displays a ball and stick diagram of tetraethylene glycol dimethyl ether (TEGDE). The figure shows TEGDE in an all trans configuration. Detailed calculations show that its structure in water is somewhat more compact.<sup>35</sup> The polymer poly(ethylene oxide) (PEO) is a technologically important polymer with a wide range of applications including ion-exchange membranes, protein crystallization, and medical devices. PEO differs from TEGDE

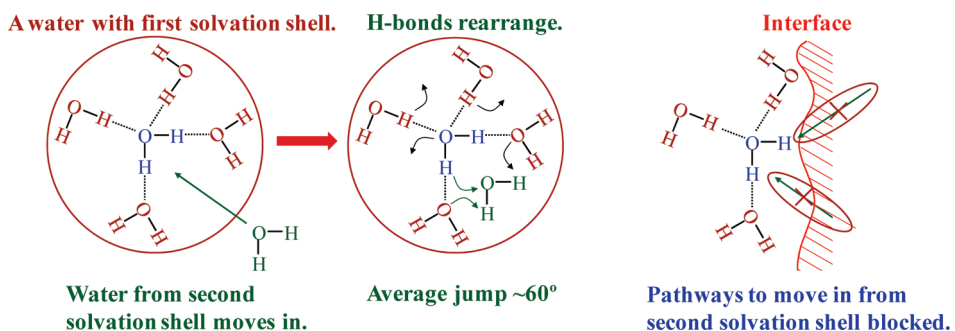


**FIGURE 10.** A schematic illustration of how an interface slows water orientational relaxation. Left-hand side, a central water with its first solvation shell. Another water moves in from the second solvation shell. Center, hydrogen bonds undergo concerted rearrangement. The central water reorients through jump reorientation. Right-hand side, An interface blocks many of the pathways necessary for jump reorientation.

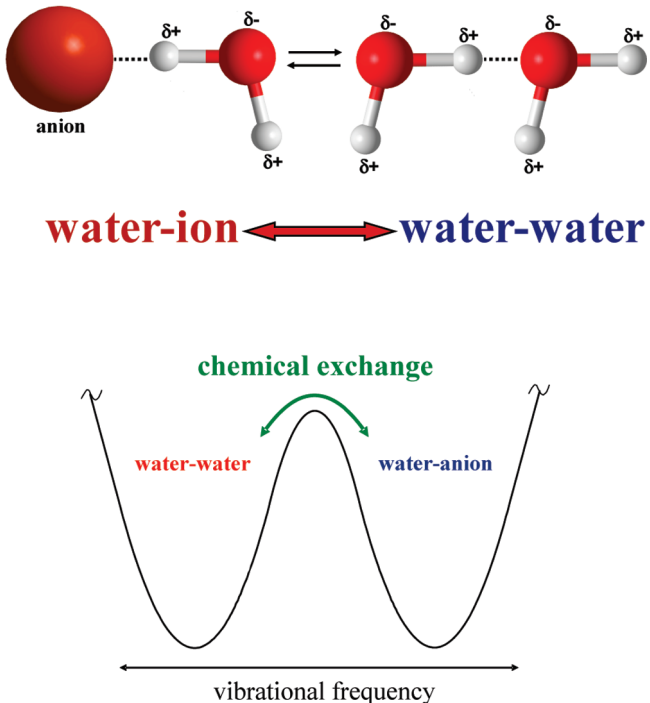
in that it has hydroxyl end groups rather than methyls. TEGDE permits the interactions of water with the ether moieties, which can act as hydrogen bond acceptors, and the nominally hydrophobic portions of the molecule to be studied without the presence of the strong interactions of water with terminal hydroxyls.<sup>13</sup> Orientation relaxation of water interacting with individual TEGDE molecules was studied over a wide range of ratios of the water to TEGDE concentrations. The lower portion of Figure 9 shows orientation relaxation of a solution of 50 water molecules per TEGDE as well as the orientational relaxation of bulk water for comparison. The water/TEGDE samples were analyzed in the same manner as discussed above using eq 6. The dashed blue curve through the TEGDE data is a fit. Data over a wide range of concentrations at a several wavelengths for each sample were fit to determine the orientational relaxation time of water interaction with TEGDE.<sup>13</sup> The results yield an orientational relaxation time of  $19 \pm 4$  ps, with individual fits ranging from 12 to 25 ps.<sup>13</sup> Like the results for water interacting with AOT reverse micelle interfaces, AOT lamellar interfaces, and Igepal reverse micelle interfaces, the orientational relaxation is significantly slower than bulk water (2.6 ps). The measured orientational relaxation times in all four systems are very similar. This again indicates that the presence of an interface or large molecule is more important than its chemical nature or geometry.

Figure 10 shows a cartoon of how water undergoes orientational relaxation in bulk water and the role that an interface plays in slowing the reorientation. The figure is a very qualitative illustration in two dimensions of what are really three-dimensional structures and processes. In bulk water, orientational relaxation involves concerted hydrogen bond rearrangement that results in jump reorientation.<sup>3,32</sup> In the left portion of the figure, a central water is shown making four hydrogen bonds to its first solvation shell. A fifth water

moves in from the second solvation shell. This additional water allows switching of a number of hydrogen bonds without leaving dangling bonds for any length of time, as shown in the middle portion of the figure. As indicated by the arrows, in switching hydrogen bonds, the central water (as well as the other waters) will change orientation. This is the jump in orientation that averages  $\sim 60^\circ$ .<sup>3,32</sup> The right-hand portion of the figure suggests the role that an interface or large molecule plays. The interface blocks many of the pathways for water to move into the first solvation shell, which greatly reduces the number of pathways that can give rise to jump reorientation. The interface eliminates an entire half space of water molecules. In addition, the rough surface topography of the interface also inhibits water molecules from moving into the first solvation shell along a range of paths that are approximately parallel to the interface. Thus the presence of the interface or other large blocking molecule is more important than its chemical nature.

The results presented above show that the presence of an interface reduces the rate of concerted hydrogen bond rearrangement as evidenced by the increase in the orientational relaxation time from 2.6 ps in bulk water to 15–20 ps when water is interacting with an interface or large molecule. The presence of charges at the interface does not make a major difference. A direct measurement of the rate of hydrogen bond exchange between a water molecule hydrogen bonded to an anion and a water molecule hydrogen bonded to another water molecule can be made using ultrafast 2D IR vibrational echo chemical exchange spectroscopy. Figure 11 shows a schematic illustration of the process. In a salt solution, water molecules will have hydroxyls hydrogen bonded to anions and to the oxygens of other water molecules. These two types of water molecules will be in equilibrium and undergo chemical exchange. If the exchange results in a sufficient change in the vibrational

## Solvation Shell Exchange



**FIGURE 11.** Schematic illustration of hydrogen bond switching between water hydrogen bonded to an anion and water hydrogen bonded to another water.

frequency, as illustrated in the bottom portion of the figure, then 2D IR chemical exchange spectroscopy can be employed to measure the time for hydrogen bond switching.<sup>8,28</sup>

Two-dimensional IR chemical exchange experiments were conducted on concentrated solutions of sodium tetrafluoroborate ( $\text{NaBF}_4$ ). An illustration of a water hydrogen bonded to a  $\text{BF}_4^-$  anion is shown in the top portion of Figure 12. The bottom portion shows the absorption spectrum of the OD stretch of dilute HOD in a  $\text{NaBF}_4$ /water solution. The peak on the blue side of the spectrum is the OD stretch when bound to the anion as shown by its increase as the  $\text{NaBF}_4$  concentration is increased.

Figure 13 shows a schematic illustration of spectra for an ideal 2D IR chemical exchange experiment. There are two species, A and B, with absorption frequencies,  $\omega_A$  and  $\omega_B$ . At short time (top panel), prior to any chemical exchange, there are two peaks on the diagonal that arise from the 0–1 vibrational transition (red, positive going), and there are two corresponding peaks below them that occur from vibrational echo emission at the 1–2 transition frequency (blue, negative going). The 1–2 peaks are shifted to lower frequency along the  $\omega_m$  axis by the amount of the vibrational anharmonicity. At long time (bottom panel), chemical

## Sodium tetrafluoroborate ( $\text{NaBF}_4$ )

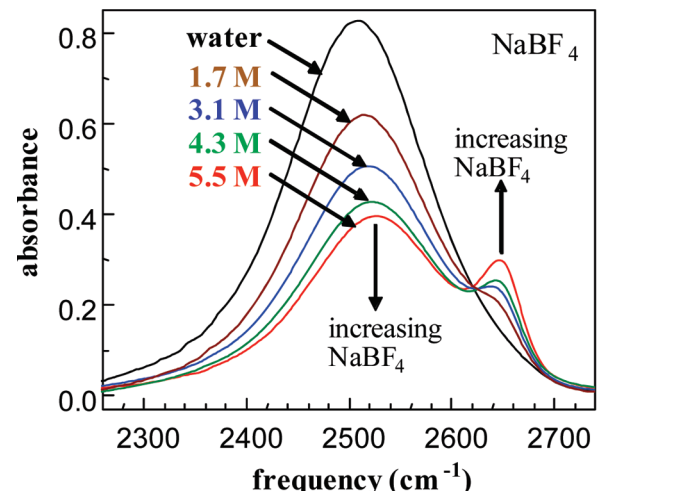
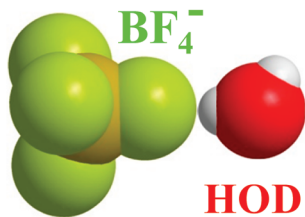


**FIGURE 12.** A schematic of a water bound to a tetrafluoroborate anion and the concentration dependent OD hydroxyl stretch spectrum of  $\text{NaBF}_4$ /water solutions.

exchange has occurred. Some A's have turned into B's, and the same number of B's have turned into A's because the system is in equilibrium. The chemical exchange is manifested by the growth of the off-diagonal peaks. Measurement of the time-dependent increase in the off-diagonal peaks, accounting for the vibrational lifetime and orientational relaxation, which causes all peaks to decrease in amplitude, gives the time dependence of the chemical exchange.<sup>28</sup>

In the schematic shown in Figure 13, the anharmonicity is large enough that the positive 0–1 peaks do not overlap with the negative 1–2 peaks. For the  $\text{NaBF}_4$ /water chemical exchange experiments, the anharmonicity of the OD hydroxyl bound to an anion ( $ha$ ) is much smaller than the anharmonicity of the hydroxyl bound to a water oxygen ( $hw$ ). Therefore, positive and negative going peaks overlap as the off-diagonal chemical exchange peaks grow in. Figure 14A shows the 2D IR spectrum at short time (200 fs) at which no chemical exchange has occurred. The peaks on the diagonal are the 0–1 positive going  $ha$  and  $hw$  peaks. The negative going 1–2  $ha$  peak is below the diagonal  $ha$  peak. The negative going 1–2  $hw$  peak is not shown. In Figure 14B, the

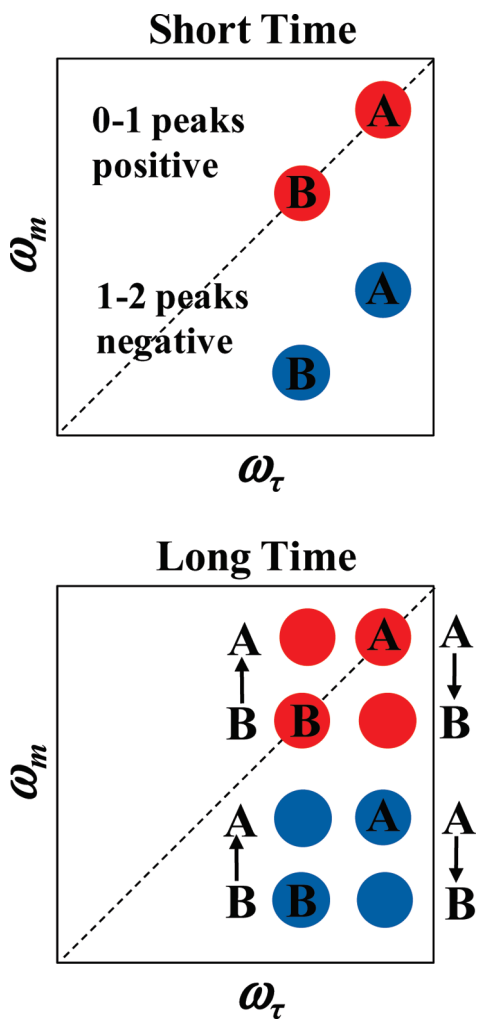


**FIGURE 13.** A schematic illustration of the effect of chemical exchange on the 2D IR vibrational echo spectrum. Chemical exchange between species A and B causes off-diagonal peaks to grow in.

spectrum is shown at 4 ps. It is very different because of chemical exchange. The off-diagonal positive exchange peak to the left of the *ha* peak and above the *hw* peak can be clearly seen. The corresponding positive exchange peak that would be below the *ha* peak and to the right of the *hw* peak is on top of the negative going 1–2 *ha* peak. In addition, one of the negative going 1–2 exchange peaks appears right in the middle of the positive going diagonal 0–1 *hw* peaks. It is manifested by essentially negating the center of the diagonal 0–1 *hw* peak. Despite the overlapping peaks, the chemical exchange data can be readily analyzed because exactly where all of the peaks will appear is known.<sup>8</sup>

Figure 14C shows the results (points) of the analysis of 2D IR spectra taken over a range of  $T_w$ 's. The diagonal peaks decay because of chemical exchange, population relaxation, and orientational relaxation. The off-diagonal peaks

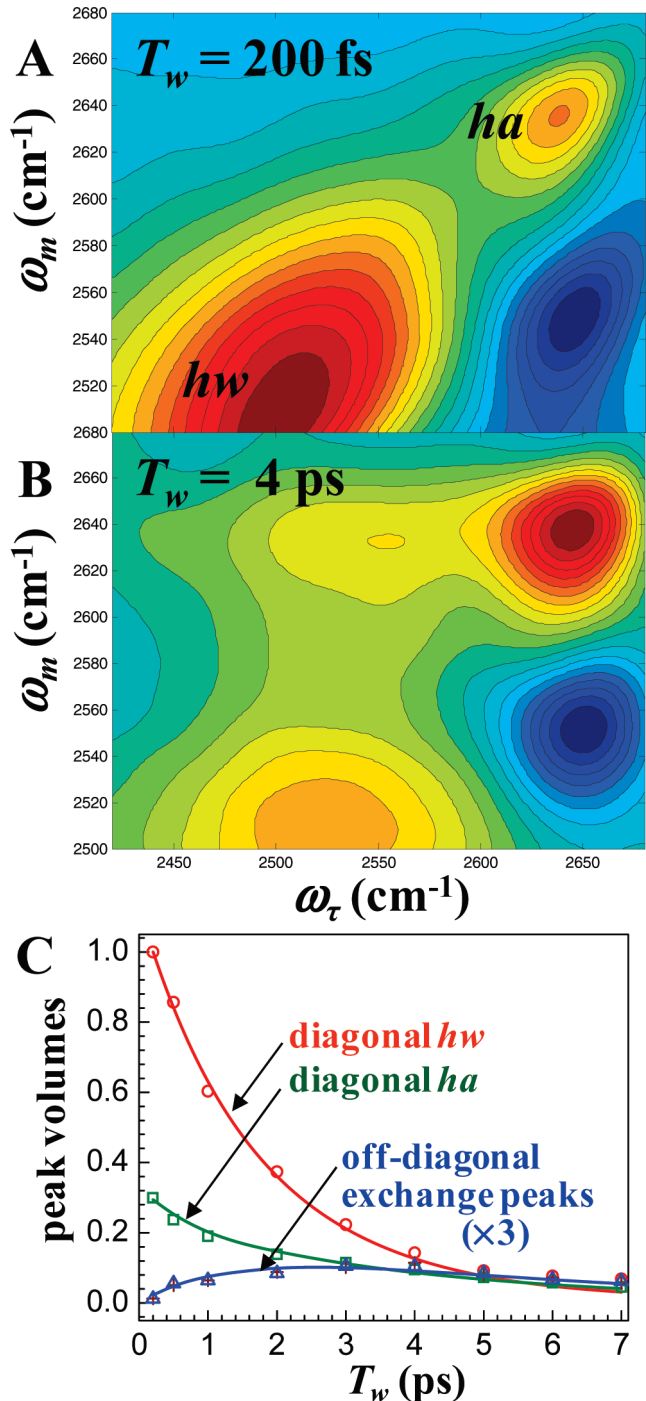


**FIGURE 14.** (A) Short time prior to chemical exchange. (B) Long time after significant chemical exchange. The appearance of overlapping positive and negative off-diagonal chemical exchange peaks causes the spectrum to change. (C) Results of the analysis of the time dependence of the 2D IR chemical exchange spectra. Points, data; solid curves, single adjustable parameter fit that yields the hydroxyl/anion (*ha*) to hydroxyl/water (*hw*) exchange time of 7 ps.

grow in because of chemical exchange but decay because of the other processes. The solid curves through the data are the result of a single adjustable parameter fit that yields the

chemical exchange time. The analysis yields the time for a water molecule hydrogen bonded to a  $\text{BF}_4^-$  anion to switch to being bonded to a water oxygen. The exchange time is 7 ps.<sup>8</sup> This should be compared with the hydrogen bond exchange time in pure water of  $\sim 2$  ps obtained from 2D IR measurements of spectral diffusion.<sup>1,4</sup> The important point is that ions slow the rearrangement of hydrogen bonds but only by a factor of 3 or 4. The relatively mild effect of ions on hydrogen bond switching may account for the relatively small difference between the interfacial dynamics of water in contact with charged vs neutral interfaces.

#### IV. Concluding Remarks

Studies using ultrafast IR spectroscopy of the dynamics of water interacting with charged vs neutral interfaces, spherical vs planar interfaces, ions, and large molecules were discussed. Water interacting with interfaces, ions, and molecules slows hydrogen bond dynamics substantially as evidence by changes in orientational relaxation times and chemical exchange dynamics. The orientational relaxation time of bulk water is 2.6 ps, which slows to  $\sim 15$ –20 ps when water interacts with a variety of interfaces or a large molecule. The most important observation is that the presence of an interface is more important in slowing hydrogen bond dynamics than the chemical nature or geometry of the interface. Current studies are examining a wide variety of additional water-containing systems.

---

This work was supported by the DOE (Grant DE-FG03-84ER13251), the NSF (Grant DMR 0652232), and the NIH (Grant 2-R01-GM061137-09).

---

#### BIOGRAPHICAL INFORMATION

**Michael D. Fayer** received his B.S. (1969) and Ph.D. (1974) from the University of California at Berkeley. He joined the faculty at Stanford University in 1974, where he is the David Mulvane Ehrensam and Edward Curtis Franklin Professor of Chemistry. He is a member of the National Academy of Science, and he has received the E. Bright Wilson Award for Spectroscopy, the Ellis R. Lippincott Award, and the Earl K. Plyler Prize for Molecular Spectroscopy.

---

#### REFERENCES

- Asbury, J. B.; Steinel, T.; Stromberg, C.; Corcelli, S. A.; Lawrence, C. P.; Skinner, J. L.; Fayer, M. D. Water Dynamics: Vibrational Echo Correlation Spectroscopy and Comparison to Molecular Dynamics Simulations. *J. Phys. Chem. A* **2004**, *108*, 1107–1119.
- Fecko, C. J.; Loparo, J. J.; Roberts, S. T.; Tokmakoff, A. Local Hydrogen Bonding Dynamics and Collective Reorganization in Water: Ultrafast Infrared Spectroscopy of  $\text{HOD}/\text{D}_2\text{O}$ . *J. Chem. Phys.* **2005**, *122*, No. 054506.
- Laage, D.; Hynes, J. T. A Molecular Jump Mechanism of Water Reorientation. *Science* **2006**, *311*, 832–835.
- Asbury, J. B.; Steinel, T.; Kwak, K.; Corcelli, S.; Lawrence, C. P.; Skinner, J. L.; Fayer, M. D. Dynamics of Water Probed with Vibrational Echo Correlation Spectroscopy. *J. Chem. Phys.* **2004**, *121*, 12431–12446.
- Fecko, C. J.; Eaves, J. D.; Loparo, J. J.; Tokmakoff, A.; Geissler, P. L. Local and Collective Hydrogen Bond Dynamics in the Ultrafast Vibrational Spectroscopy of Liquid Water. *Science* **2003**, *301*, 1698–1702.
- Hamm, P.; Lim, M.; Hochstrasser, R. M. Non-Markovian Dynamics of the Vibrations of Ions in Water from Femtosecond Infrared Three-Pulse Photon Echoes. *Phys. Rev. Lett.* **1998**, *81*, 5326–5329.
- Heyne, K.; Nibbering, E. T. J.; Elsaesser, T.; Petkovic, M.; Kuhn, O. Cascaded Energy Redistribution Upon O-H Stretching Excitation in an Intramolecular Hydrogen Bond. *J. Phys. Chem. A* **2004**, *108*, 6083–6086.
- Moilanen, D. E.; Wong, D. B.; Rosenfeld, D. E.; Fenn, E. E.; Fayer, M. D. Ion-Water Hydrogen Bond Switching Observed with 2D IR Vibrational Echo Chemical Exchange Spectroscopy. *Proc. Natl. Acad. Sci. U.S.A.* **2009**, *106*, 375–380.
- Moilanen, D. E.; Fenn, E. E.; Lin, Y.-S.; Skinner, J. L.; Bagchi, B.; Fayer, M. D. Water Inertial Reorientation: Hydrogen Bond Strength and the Angular Potential. *Proc. Natl. Acad. Sci. U.S.A.* **2008**, *105*, 5295–5300.
- Moilanen, D. E.; Fenn, E. E.; Wong, D. B.; Fayer, M. D. Water Dynamics in Large and Small Reverse Micelles: From Two Ensembles to Collective Behavior. *J. Chem. Phys.* **2009**, *131*, 014704.
- Moilanen, D. E.; Fenn, E. E.; Wong, D. B.; Fayer, M. D. Geometry and Nanolength Scales vs. Interface Interactions: Water Dynamics in AOT Lamellar Structures and Reverse Micelles. *J. Am. Chem. Soc.* **2009**, *131*, 8318–8328.
- Moilanen, D. E.; Fenn, E. E.; Wong, D. B.; Fayer, M. D. Water Dynamics at the Interface in AOT Reverse Micelles. *J. Phys. Chem. B* **2009**, *113*, 8560–8568.
- Fenn, E. E.; Moilanen, D. E.; Levinger, N. E.; Fayer, M. D. Water Dynamics and Interactions in Water–Polyether Binary Mixtures. *J. Am. Chem. Soc.* **2009**, *131*, 5530–5539.
- Piletic, I. R.; Moilanen, D. E.; Spry, D. B.; Levinger, N. E.; Fayer, M. D. Testing the Core/Shell Model of Nanoconfined Water in Reverse Micelles Using Linear and Nonlinear IR Spectroscopy. *J. Phys. Chem. A* **2006**, *110*, 4985–4999.
- Piletic, I. R.; Moilanen, D. E.; Levinger, N. E.; Fayer, M. D. What Nonlinear-IR Experiments Can Tell You About Water That the IR Spectrum Cannot. *J. Am. Chem. Soc.* **2006**, *128*, 10366–10367.
- Bakker, H. J.; Kropman, M. F.; Omata, Y.; Woutersen, S. Hydrogen-Bond Dynamics of Water in Ionic Solutions. *Phys. Scr.* **2004**, *69*, C14–C24.
- Dokter, A. M.; Woutersen, S.; Bakker, H. J. Anomalous Slowing Down of the Vibrational Relaxation of Liquid Water Upon Nanoscale Confinement. *Phys. Rev. Lett.* **2005**, *94*, No. 178301.
- Park, S.; Fayer, M. D. Hydrogen Bond Dynamics in Aqueous NaBr Solutions. *Proc. Natl. Acad. Sci. U.S.A.* **2007**, *104*, 16731–16738.
- Fenn, E. E.; Wong, W.; Fayer, M. D. Water Dynamics at Neutral and Ionic Interfaces in Reverse Micelles. *Proc. Natl. Acad. Sci. U.S.A.* **2009**, *106*, 15243–15248.
- Moilanen, D. E.; Levinger, N.; Spry, D. B.; Fayer, M. D. Confinement or Properties of the Interface? Dynamics of Nanoscopic Water in Reverse Micelles. *J. Am. Chem. Soc.* **2007**, *129*, 14311–14318.
- Moilanen, D. E.; Piletic, I. R.; Fayer, M. D. Tracking Water's Response to Structural Changes in Nafion Membranes. *J. Phys. Chem. A* **2006**, *110*, 9084–9088.
- Moilanen, D. E.; Piletic, I. R.; Fayer, M. D. Water Dynamics in Nafion Fuel Cell Membranes: The Effects of Confinement and Structural Changes on the Hydrogen Bond Network. *J. Phys. Chem. C* **2007**, *111*, 8884–8891.
- Woutersen, S.; Bakker, H. J. Resonant Intermolecular Transfer of Vibrational Energy in Liquid Water. *Nature (London)* **1999**, *402*, 507–509.
- Gaffney, K. J.; Piletic, I. R.; Fayer, M. D. Orientational Relaxation and Vibrational Excitation Transfer in Methanol - Carbon Tetrachloride Solutions. *J. Chem. Phys.* **2003**, *118*, 2270–2278.
- Park, S.; Kwak, K.; Fayer, M. D. Ultrafast 2D-IR Vibrational Echo Spectroscopy: A Probe of Molecular Dynamics. *Laser Phys. Lett.* **2007**, *4*, 704–718.
- Kwak, K.; Park, S.; Finkelstein, I. J.; Fayer, M. D. Frequency-Frequency Correlation Functions and Apodization in 2D-IR Vibrational Echo Spectroscopy, a New Approach. *J. Chem. Phys.* **2007**, *127*, No. 124503.
- Kwak, K.; Rosenfeld, D. E.; Fayer, M. D. Taking Apart 2D-IR Vibrational Echo Spectra: More Information and Elimination of Distortions. *J. Chem. Phys.* **2008**, *128*, No. 204505.
- Zheng, J.; Kwak, K.; Asbury, J. B.; Chen, X.; Piletic, I.; Fayer, M. D. Ultrafast Dynamics of Solute-Solvent Complexation Observed at Thermal Equilibrium in Real Time. *Science* **2005**, *309*, 1338–1343.
- Kwak, K.; Zheng, J.; Cang, H.; Fayer, M. D. Ultrafast 2D IR Vibrational Echo Chemical Exchange Experiments and Theory. *J. Phys. Chem. B* **2006**, *110*, 19998–20013.

- 30 Zulauf, M.; Eicke, H.-F. Inverted Micelles and Microemulsions in the Ternary System Water/Aerosol-OT/Isooctane as Studied by Photon Correlation Spectroscopy. *J. Phys. Chem.* **1979**, *83*, 480–486.
- 31 Cringus, D.; Bakulin, A.; Lindner, J.; Vohringer, P.; Pshenichnikov, M. S.; Wiersma, D. A. Ultrafast Energy Transfer in Water-AOT Reverse Micelles. *J. Phys. Chem. B* **2007**, *111*, 14193–14207.
- 32 Laage, D.; Hynes, J. T. On the Molecular Mechanism of Water Reorientation. *J. Phys. Chem. B* **2008**, *112*, 14230–14242.
- 33 Fontell, K. The Structure of the Lamellar Liquid Crystalline Phase in Aerosol OT-Water System. *J. Colloid Interface Sci.* **1973**, *44*, 318–329.
- 34 Lippens, S.; Schubel, D.; Schlicht, L.; Spilgies, J.-H.; Ilgenfritz, G.; Eastoe, J.; Heenan, R. K. Percolation in Nonionic Water-in-Oil-Microemulsion Systems: A Small Angle Neutron Scattering Study. *Langmuir* **1998**, *14*, 1041–1049.
- 35 Sturlaugson, A. L.; Fruchey, K. S.; Lynch, S. R.; Aragón, S. R.; Fayer, M. D. Orientational and Translational Dynamics of Polyether/Water Solutions. *J. Phys. Chem. B* **2010**, *114*, 5350–5358.